The 14th International Topical Meeting on Nuclear Reactor Thermalhydraulics, NURETH-14
Toronto, Ontario, Canada, September 25-30, 2011

NURETH14-636

DEVELOPMENT OF INTERFACIAL AREA TRANSPORT EQUATION – MODELING AND EXPERIMENTAL BENCHMARK

M. Ishii[1]
[1] Purdue University, West Lafayette, Indiana, USA

Abstract

A dynamic treatment of interfacial area concentration has been studied over the last decade by employing the interfacial area transport equation. When coupled with the two-fluid model, the interfacial area transport equation replaces the flow regime dependent correlations for interfacial area concentration and eliminates potential artificial bifurcation or numerical oscillations stemming from these static correlations. An extensive database has been established to evaluate the model under various two-phase flow conditions. These include adiabatic and heated conditions, vertical and horizontal flow orientations, round, rectangular, annulus and 8×8 rod bundle channel geometries, and normal-gravity and simulated reduced-gravity conditions. This paper reviews the current state-of-the-art in the development of the interfacial area transport equation, available experimental databases and 1D and 3D benchmarking work of the interfacial area transport equation.

Introduction

An accurate prediction of two-phase flow, either under a steady state or transient condition is very important for the design, operation and analysis of complicated industrial systems such as a nuclear reactor coolant system. Two-phase flow in the nuclear reactor generally involves a wide spectrum of scales ranging from the micro scale phenomena (<1mm) such as bubble nucleation and condensation, to the system scale in the order of 10m or larger. Due to its complicated nature, the most practical two-phase flow model that has sufficient details yet is simple enough to obtain transient solutions is the well-known two-fluid model. The two-fluid model is obtained by averaging the single phase field equations of each phase to remove the high frequency spatial and temporal fluctuations. In this way, local instantaneous quantities of fluids, such as variations of pressure, velocity and temperature inside a bubble or a droplet, are not explicitly considered. The averaged quantities such as volume fraction of bubbles, averaged gas and liquid velocities, and averaged pressure appear as unknowns in the field equations in the two-fluid model. The distinct features associated to the interface are smeared off during the averaging process. The interfacial transfer terms arise in the field equations to account for the interactions between two phases.

For most two-phase flows under consideration, the interfacial transfer terms are as important (if not more than) as the turbulent terms. The interfacial transfer terms strongly depend on the

interfacial structures. To quantify the interfacial structure impact on the interfacial transfer terms, the interfacial area concentration a_i is defined as the surface area per unit two-phase mixture volume. It can be shown that the interfacial mass, momentum and heat transfer rates are all dependent on a_i. Therefore, the interfacial area concentration is a key parameter in solving the two-fluid model.

The present thermal-hydraulic system analysis codes such as RELAP5, TRAC, and CATHARE use one-dimensional form of the two-fluid model equations, where the interfacial area concentration is specified by empirical correlations based on steady-state, fully developed conditions. This approach has many shortcomings since flow regime is a qualitative description and it is often rather subjective. It cannot handle the dynamic development of two-phase flow structures such as entrance effect, flow near the transition boundary, and flow structure with strong multi-dimensional distributions. When applied to system analysis code, the flow regime dependent correlations may induce numerical oscillations and instabilities due to the artificial bifurcation of these models.

In view of the above, the interfacial area transport equation (IATE) was developed by Kocamustafaogullari and Ishii [1] based on the concept of particle number density distribution. This approach starts from the Boltzmann transport equation which describes the statistical characteristics of a large number of dispersed particles. The transport equation of averaged interfacial area concentration can be obtained by first weighting the Boltzmann equation with the surface area of each particle, and then taking the integration over the entire particle volume range. The IATE can model the evolution of interfacial structures across the flow regime transition boundaries through mechanistic modeling of various fluid particle interaction phenomena. Therefore, using IATE to predict the interfacial area concentration is not only more accurate and consistent with the two-fluid model, but also eliminates the artificial discontinuities stemming from the use of flow regime dependent correlations.

In this paper, the formulation of IATE from the Boltzmann transport equation and modeling of various source/sink terms are first reviewed. In section 2, the instrumentation used for interfacial area measurement and the available experimental database are presented. Finally, sample 1D and 3D benchmarking results are discussed in section 3.

1. Formulation of interfacial area transport equation

1.1 Two-group interfacial area transport equation

The foundation of the IATE was established based on the Boltzmann transport equation of the particle number densities for dispersed two-phase systems [1]. Let $f(\vec{x},V,t)$ be the particle number density distribution function per unit mixture volume. This is assumed to be continuous and specifies the probable number density of fluid particles moving at a given time t, in a spatial range $\delta\vec{x}$ with its center-of-volume located at $\vec{x}$ with particle volumes between V and $V + \delta V$. The kinetic theory gives the following transport equation of particle number density distribution f:

$$\frac{\partial f}{\partial t}+\nabla\cdot\left(f\vec{v}\right)+\frac{\partial}{\partial V}\left(f\frac{dV}{dt}\right)=\sum_j S_j+S_{ph}\ . \tag{1}$$

In the right-hand side (RHS) of the equation, the S_j and S_{ph} terms are the particle source and sink rates per unit mixture volume due to j^{th} particle interactions (such as the disintegration or coalescence) and that due to phase change, respectively. By multiplying the above equation by the surface area of particles with volume V, and then integrating over the entire particle volume range, one can obtain the macroscopic transport equation of a_i [1]:

$$\frac{\partial a_i}{\partial t}+\nabla\cdot\left(a_i\vec{v}_i\right)-\frac{2}{3}\left(\frac{a_i}{\alpha_g}\right)\left\{\frac{\partial\alpha_g}{\partial t}+\nabla\cdot\left(\alpha_g\vec{v}_g\right)-\eta_{ph}\right\}=\sum_j\phi_j+\phi_{ph}\ . \tag{2}$$

The first two terms in the LHS of Eq. (2) represent the time rate of change of a_i and its convection. The other terms are divided into two categories based on their mechanisms to alter interfacial area: volume change term as the third one in the LHS and number density change terms in the RHS of the equation. In the volume change term, the volume source from nucleation or condensation η_{ph} is excluded from the total void fraction change. This is because η_{ph} comes with bubble number density change and it is considered in the term ϕ_{ph}. The ϕ_j's and ϕ_{ph} in the RHS of Eq. (2) represent the rate of change in the interfacial area concentration due to particle interactions and that due to phase change, respectively.

In typical two-phase flows, a large amount of bubbles exist in various sizes and shapes. These variations cause substantial differences in the hydrodynamic behaviors such as drag, lift and wall forces, as well as the bubble interaction mechanisms. For most two-phase flows, bubbles can be classified into five types [2]: spherical, distorted, cap, slug and churn-turbulent bubbles. Based their geometric and hydrodynamic characteristics, they can be divided into two major groups, such that group 1 includes spherical and distorted bubbles, while group 2 consists of cap, slug and churn-turbulent bubbles. For typical industrial systems such as nuclear power plants, the length scale of group 2 bubbles is usually comparable to or even larger than the flow duct. Therefore geometric effect of the flow duct should be considered in developing the hydrodynamic and interfacial closures. This is not necessary for group 1 bubbles as the length scale is usually much smaller than that of flow duct. The boundary between the two groups is given by the maximum distorted bubble limit [2] $D_{d,\max}=4\sqrt{\sigma/g\Delta\rho}$, where, σ, $\Delta\rho$ and g are surface tension, density difference and gravitational acceleration, respectively.

Given the above bubble classification and group boundary, the two group IATE can be obtained in the similar way as the one group IATE [3]:

$$\frac{\partial a_{i1}}{\partial t}+\nabla\cdot\left(a_{i1}\vec{v}_{i1}\right)=\left(\frac{2}{3}-C\left(\frac{D_{sc}}{D_{Sm1}}\right)^2\right)\frac{a_{i1}}{\alpha_1}\left[\frac{\partial\alpha_1}{\partial t}+\nabla\cdot\left(\alpha_1\vec{v}_{g_1}\right)-\eta_{ph}\right]+\sum_j\phi_{j,1}+\phi_{ph}\ , \tag{3}$$

and

$$\frac{\partial a_{i2}}{\partial t}+\nabla\cdot\left(a_{i2}\vec{v}_{i2}\right)=\frac{2}{3}\frac{a_{i2}}{\alpha_2}\left[\frac{\partial\alpha_2}{\partial t}+\nabla\cdot\left(\alpha_2\vec{v}_{g_2}\right)\right]+C\left(\frac{D_{sc}}{D_{Sm1}}\right)^2\frac{a_{i1}}{\alpha_1}\left[\frac{\partial\alpha_1}{\partial t}+\nabla\cdot\left(\alpha_1\vec{v}_{g_1}\right)-\eta_{ph}\right]+\sum_j\phi_{j,2}\ . \tag{4}$$

Here D_{sc} is the surface area equivalent diameter at the group boundary. The constant C is a coefficient to quantify the magnitude of inter-group transfer. It can be seen that the same inter-group transfer term arises in both equations with opposite signs. Therefore the inter-group transfer terms vanish if adding equations (3) and (4) together, which is consistent with the form of one-group IATE. It is also noticed that the nucleation and condensation terms η_{ph} and ϕ_{ph} are excluded from the group 2 equation, given that small nucleation and condensation bubbles generally fall in group 1 category.

Equations (2), (3) and (4) compose the basic field equations of the one group and two group IATEs. The source and sink terms should be correctly modeled to account for various particle interaction and phase change mechanisms.

1.2 Modeling of interfacial source/sink terms

Bubble interaction, either coalescence or breakup, largely exists in both adiabatic and diabatic two-phase flows. The flow regime transitions are usually caused by various bubble interactions. Therefore, the bubble interactions play very important roles in the development of interfacial structures and they must be properly modeled to close the IATE. There are generally two approaches to develop source and sink terms caused by various bubble interaction mechanisms: considering the algebraic equation of the particle mean parameters (or assuming monosized particles); and solving the integral equation with particle size distributions. In the first approach, the source term is simplified as [3]:

$$\phi_j\equiv S_j\Delta A_i\ . \tag{5}$$

Here S_j is the particle number source and sink rate due to j^{th} interaction mechanism. ΔA_i is the surface area change during one particle interaction event. It is assumed that each coalescence and breakup event is a binary process which only involves two particles of the same size.

The monosized particle approach greatly simplifies the process to develop the source and sink closures. However, it is not proper for the two-group IATE, where the sizes of group 2 bubbles have much larger variations compared to group 1 bubbles. In this case, the approach based on the integration over bubble distribution should be adopted in developing source and sink closures. For a coalescence mechanism, bubble number density gain rate S_{GC} can be given for the bubbles with volume V as [1, 4]:

$$S_{GC}\left(V\right)=\int_{V_{\min}}^{V/2}\lambda\left(V-V',V'\right)h\left(V-V',V'\right)f\left(V-V'\right)f\left(V'\right)dV'\ , \tag{6}$$

where $h(V\text{-}V',V')$ and $\lambda(V\text{-}V',V')$ are the collision frequency and coalescence efficiency of bubbles of volume $V\text{-}V'$ and V'. Similarly, the loss rate due to the same coalescence mechanism S_{LC} can be written as:

$$S_{LC}(V) = -\int_{V_{\min}}^{V_{\max}-V} \lambda(V,V')h(V,V')\, f(V)\, f(V')\, dV' \,. \tag{7}$$

Given the surface area A_i of the particle with volume V, the interfacial area source or sink term can be obtained by integrating the A_i weighted particle number density gain or loss rate:

$$\phi_j = \int_{V_{\min}}^{V_{\max}} S(V)\, A_i(V)\, dV \,. \tag{8}$$

The net change rate of particle number density is the sum of the gain and loss rate. For example, the bubble coalescence results in gain of large bubbles and loss of small bubbles. The net change of interfacial area is the combination of these two opposite effects. In practice, one must also consider the particular interaction mechanism and proper classification of the two groups.

During the past studies over a wide range of two-phase flow conditions, a number of bubble coalescence and breakup mechanisms have been identified. Among them, the random collision, wake entrainment, turbulent impact, shearing off and surface instability, were considered to be important for most two-phase flows and the mechanistic models have been developed for these mechanisms [5].

2. Interfacial area measurement and database

2.1 Local multi-sensor probes

The local time-averaged interfacial area concentration can be measured using various local conductivity or optical probes [6, 7]. A four-sensor conductivity probe method based on the difference in conductivity between the two phases has been widely used in various two-phase flow conditions up to churn-turbulent flow regime [6]. One of the most important features of the four-sensor conductivity probe is that it can measure the local interfacial velocity. This is of great importance because the local time-averaged interfacial area concentration can be obtained from the interfacial velocity through the mathematical relation [6],

$$a_i = \frac{1}{\Omega}\sum_j \sqrt{\left(\frac{1}{v_{s1j}}\right)^2 + \left(\frac{1}{v_{s2j}}\right)^2 + \left(\frac{1}{v_{s3j}}\right)^2} \,, \tag{9}$$

where Ω is time interval and v_{skj} is the passing velocity of the j^{th} interface over sensor k. In the above equation, no hypothesis for bubble shape is needed for calculating the local interfacial area concentration from the interfacial velocity. Therefore, the four-sensor probe can be utilized in a wide range of two-phase flow regimes where bubbles are no longer

spherical in shape. If we consider spherical bubbly flow with no correlation between bubble velocity and moving direction, Eq.(9) can be simplified to enable double sensor probe method to measure the interfacial area concentration [8].

To minimize the finite probe size effect on the measurement, a miniaturized four-sensor conductivity probe has been developed [9]. This four sensor probe design accommodates a built-in double-sensor probe for measuring small bubbles. Therefore, the probe is applicable to a wide range of flow regimes, spanning from bubbly to churn-turbulent flow regimes. Along with the probe design, the signal processing is constructed, such that it can identify and separate the local parameters into two groups, namely: group-1 for spherical and distorted bubbles and group-2 for slug and churn-turbulent bubbles. The measurement area of the four-sensor probe used in the experiments is less than 0.2 mm^2 and the tip distance of the double-sensor probe for small bubbles is 2.4 mm. This allows the measurable bubble diameter to be as smal1 as 1 mm. The details of the double sensor and four-sensor probe techniques can be found in reference [8] and [9].

2.2 Interfacial area database

Extensive data of axial development of flow parameters in adiabatic and boiling two-phase flow have been obtained over a wide range of flow conditions including downward flow. The measured flow parameters include local void fraction, interfacial area concentration, interfacial velocity, bubble Sauter mean diameter, liquid velocity and liquid turbulence. The covered experimental conditions are

- Test section geometry: Round pipe, confined channel, annulus and rod bundle,
- Test section size: 1 mm to 102 mm,
- Flow regime: Bubbly, cap-bubbly, slug and churn-turbulent flows,
- Flow condition: Superficial gas velocity, j_g, up to 10 m/s and superficial liquid velocity, j_f, from -3.1 m/s (i.e. downward flow) to 5.0 m/s (i.e. upward flow),
- Flow direction: Vertical upward and downward flows,
- Thermal condition: Adiabatic and diabatic flows,
- Gravity condition: Normal and micro gravity conditions,
- Pressure condition: Atmospheric pressure and elevated pressure up to 10bar.

The extensive review of the existing database can be found in the references [5, 10].

A recent interfacial area database is developed for air-water two-phase flow in an 8×8 rod bundle test facility at elevated pressures [11]. The test section is composed of a stainless steel outer casing with square cross section and side length of 140 mm. Inside the casing are 64 stainless steel rods with diameter of 10.3 mm and pitch of 16.7 mm. These values have been carefully determined by a detailed scaling analysis based on actual BWR bundle specifications. Spacer grids, which function as they do in actual reactor systems to maintain the spacing between the rods, are located in the test section at axial locations of z/D_h = 21, 42, 63, 83, 104, 123 and 143, where D_h = 2.14 cm is the subchannel hydraulic diameter and z is the distance from the test section inlet. Measurements are obtained at four locations with z/D_h = 5, 77, 85 and 137.

Sample two group void fraction and interfacial area profiles in a cap-turbulent flow regime is shown in Figure 1. Open and solid symbols indicate local flow parameter measured at subchannel center and rod narrowest gap, respectively. Circle and triangle symbols indicate local flow parameters for group-1 and -2 bubbles. As can be seen from the figure, difference in flow parameter distribution between the subchannel center and rod narrowest gap are quite noticeable. The global distribution and relative magnitude of two group parameters are similar to those found in large pipe flows. Generally, group 2 void fraction shows apparent center peaking in both subchannel and over the entire bundle cross section. Group 1 void fraction, on the other hand, has a relatively uniform distribution. The interfacial area concentration of group 1 bubbles is considerably larger than group 2 bubbles, especially near the casing wall. This is opposite to the void fraction since group 1 bubbles are much smaller than group 2. From the experiment, it is observed that group 2 bubbles can grow to be larger than the subchannel size and therefore can span multiple subchannels. This has a multitude of effects on the flow, largely resulting in a shift in the dominant length scale from the subchannel hydraulic diameter to the casing hydraulic diameter. This leads to the effect shown in the figure, where the profile across the test section is much more significant than the profiles within each subchannel.

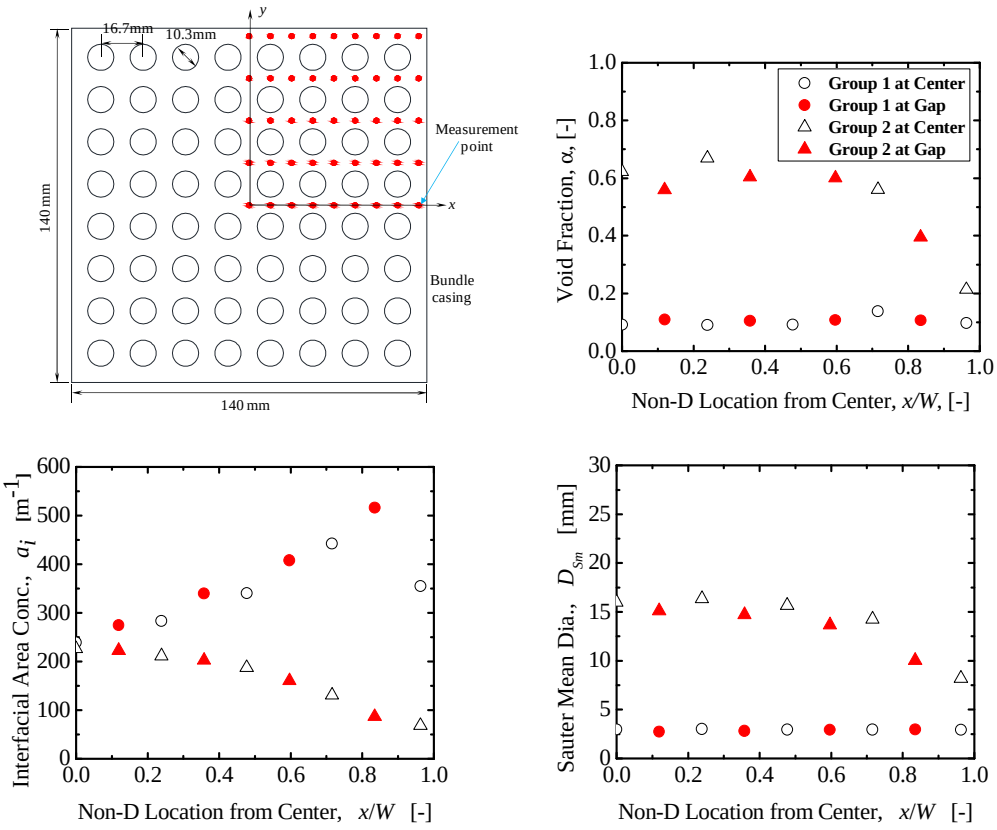

Figure 1 Local data in an 8x8 rod bundle, j_f=0.59 m/s, j_g=1.2 m/s, p=300 kPa, y=0 mm.

3. Benchmarking of IATE

3.1 Benchmarking of 1D IATE

The interfacial area transport equation has been validated against an extensive amount of data obtained in experiments under various two-phase flow conditions. Consistently throughout the evaluation studies, good agreements were found between the predictions made by the interfacial area transport equation and the experimental data. As an example, Figure 2 shows the axial interfacial area development and 1D two group IATE prediction for the cap-turbulent flow condition in the 8x8 rod bundle geometry discussed previously. The void fraction development agrees very well with the data, and the interfacial area concentration prediction is also reasonable. For Group 1, the dominant source of interfacial area concentration is bubble expansion, while dominant sinks are wake entrainment by Group 2 bubbles and, to a lesser extent, coalescence due to random collision. For Group 2 the dominant sources are bubble expansion and wake entrainment of Group 1 bubbles, with coalescence of Group 1 bubbles by random collision having a small effect. Dominant sinks for Group 2 include random collision of Group 2 bubbles and wake entrainment of Group 2 bubbles.

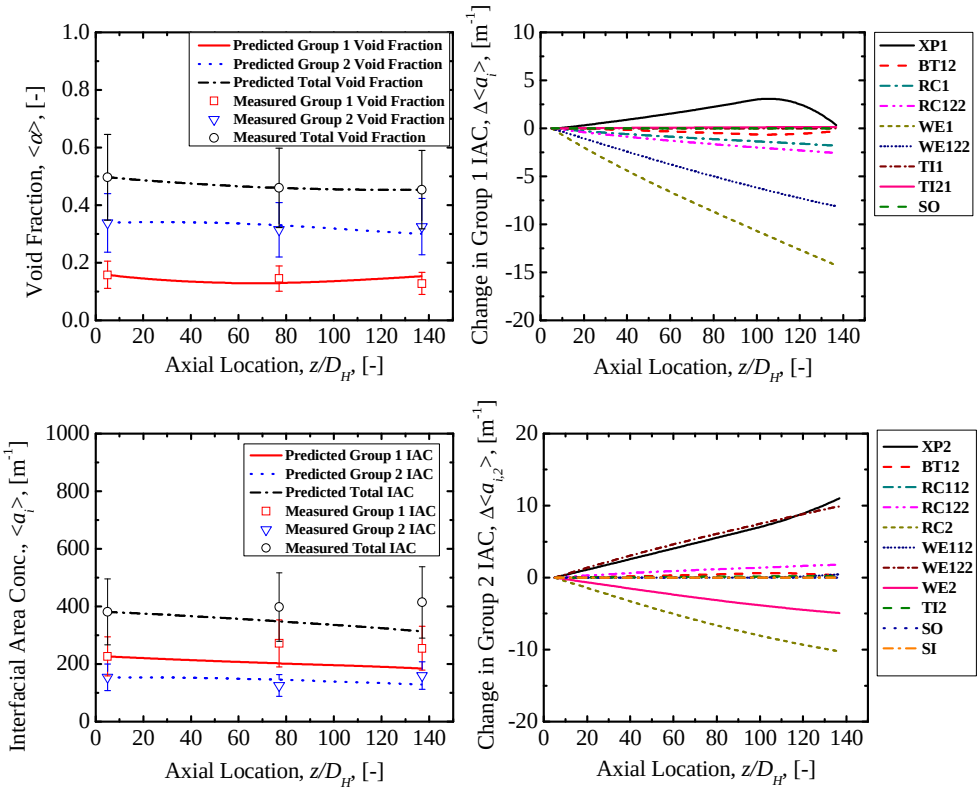

Figure 2 IATE prediction in an 8x8 rod bundle, j_f=0.59 m/s, j_g=1.2 m/s, p=300 kPa.

The one-group interfacial area transport equation is evaluated by comparison with the data obtained in both the upward and downward adiabatic and boiling two-phase flows in various sizes of pipes, in various channel geometries and in vertical and horizontal flow orientations. Some of the notable findings can be summarized as [12]: (1) The model coefficients for the

vertical upward two-phase flow in round pipe geometries remain the same regardless of the pipe sizes; (2) While the mechanisms governing the bubble coalescence remain similar regardless of the flow direction, it is clear that they were affected by the channel geometry; (3) The swirling motion of bubbles in co-current downward flow induces large scale eddies, which sweep the bubble clusters as a whole, resulting in a weaker bubble disintegration mechanism due to turbulent impact than that in the upward flow; (4) The spacer grid in the rod bundle acts as an interfacial area source or sink depending on the flow rate and flow regime; (5) The interfacial area change due to condensation is governed by inertia-controlled and thermal-controlled bubble collapse mechanisms; (6) The interfacial area transport equation formulated at normal gravity conditions may be extended to reduced-gravity conditions; and (7) geometric effects due to elbows are evident in interfacial area transport in horizontal two-phase flow, as well as the contributions from the two-phase minor loss and change in bubble velocity. In all of the above studies, the predictions made by the one-group interfacial area transport equation agree well with the experimental data within ±20% error.

The two-group interfacial area transport equation is also evaluated by a wide range of conditions in adiabatic vertical upward air-water two-phase flows in two flow channel geometries: i.e., the round pipes of various sizes and a rectangular test section. For the round pipe geometry, a comprehensive database in three different pipe sizes was established in bubbly, slug and churn-turbulent flow regimes. The pipe sizes employed for experiments were 50.8, 101.6 and 152.4 mm inner diameters. For the rectangular geometry, a test section with 10 mm×200 mm cross-sectional area was employed, and the local two-phase flow parameters were obtained in bubbly, cap-turbulent and churn-turbulent flow regimes. In total, 204 data points were evaluated for the two-phase flow in round pipes, and 71 data points were evaluated for the rectangular geometry. Accounting for the difference in flow channel geometries and their influences in bubble transport, two sets of coefficients were determined based on the experimental data. In general, the two-group model showed good agreement with the data.

3.2 Benchmarking of 3D IATE

Two-phase CFD simulation with 3D two-fluid model and IATE has been carried out by many researchers in the past decade or so. Yao and Morel [13] implemented a modified interfacial area transport equation into CATHARE, and good prediction results were observed. Yeoh and Tu [14], and Huh et al. [15] explored the possibility of applying the number density transport equation to gas-liquid two-phase flows to provide a constitutive relation for the interfacial area concentration. Recently, Wang and Sun [16, 17] implemented the interfacial area transport equation into a the commercial CFD code, FLUENT. In their study, the fully three-dimensional one-group IATE was implemented into FLUENT version 6.3.33. The capability of interfacial area transport equation was clearly demonstrated by simulating the lateral distributions of various two-phase flow parameters, including the void fraction, interfacial area concentration and the bubble Sauter mean diameter.

In the study performed by Wang and Sun [16, 17], the interfacial area concentration was introduced into FLUENT as a user-defined scalar (UDS) for the gas phase and it was

computed by the default transport equation. The interfacial area concentration was then linked with the Eulerian multiphase model through the interfacial force in the ensemble-averaged two-fluid momentum equations. When coupled with the interfacial area transport equation, the bubble size in FLUENT was calculated via the interfacial area transport equation to obtain the drag and lift coefficients, while a constant bubble diameter was used as a default in the original FLUENT code. Figures 3 shows the simulation results obtained by the conventional FLUENT code and those by FLUENT coupled with the interfacial area transport equation. The experimental data were obtained for co-current upward adiabatic bubbly flows in a round pipe of 50.8 mm inner diameter. Figures 3 (a) shows the void fraction results obtained for a test run with superficial liquid and gas velocities of j_f = 0.986 and j_g = 0.321 m/s. The measured data at the inlet of the pipe were used as the boundary conditions. In the figures, r and R are the radial distance measured from the pipe center and pipe radius, respectively. As can be seen, characteristic lateral distributions of the void fraction across the pipe radius are successfully simulated by FLUENT when it is coupled with the interfacial area transport equation. In contrast, the simulation result obtained by the conventional FLUENT (without the interfacial area transport equation) predicts a uniform void fraction distribution up to r/R = 0.8, which is different from the experimental data and not very realistic. Similar results can be found in a more turbulent flow condition of j_f = 2.34 and j_g = 0.56 m/s, where significantly more large bubbles, such as cap bubbles, exist as well as the small dispersed bubbles. It is clear from these results that the interfacial area transport equation is indispensable for CFD codes to capture the two-phase flow transport phenomena properly.

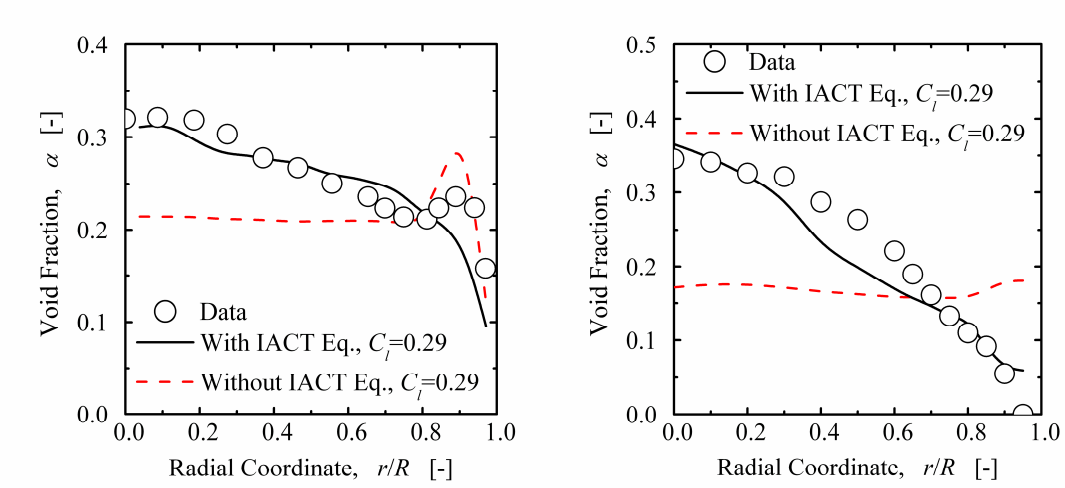

Figure 3 Comparisons of void fraction prediction with the experimental data taken for air-water upflow in a 50.8 mm pipe (a) j_f = 0.986, j_g = 0.321 m/s; (b) j_f = 2.34 and j_g = 0.56 m/s [16, 17].

4. Conclusion

A comprehensive review on the state-of-the-art in the development of the interfacial area transport equation is presented, including the model development, experimental studies and 1D and 3D model benchmarking. The interfacial area transport equation eliminates inherent shortcomings of conventional flow regime based correlations by dynamically modeling the evolution of interfacial structures via mechanistic modeling of fluid particle interactions.

Two-group transport formulations are presented which account for the characteristic differences in bubble shape, transport phenomena and bubble interaction mechanisms in a wide range of two-phase flow regimes, namely bubbly to churn-turbulent flow regimes. The group-1 equation accounts for the transport of spherical and distorted bubbles and the group-2 equation accounts for the large cap or churn-turbulent bubbles. The models are benchmarked based on an extensive database established under various two-phase flow conditions, including the adiabatic and heated conditions, vertical and horizontal flow orientations, round, rectangular, and annulus, and normal-gravity and simulated micro-gravity conditions. Recent efforts in implementing the interfacial area transport equation in CFD codes are briefly discussed. Results from these studies clearly demonstrate the capability of interfacial area transport equation in modeling two-phase flow. Use of the dynamic interfacial area transport equation is not only consistent with the use of two-fluid model, but it also provides accurate prediction for a wider range of conditions, and eliminates the numerical problems associated with the use of static empirical correlations.

5. Acknowledgement

The work presented in this paper is performed under the auspices of the U.S. Nuclear Regulatory Commission, Bettis Atomic Laboratory, the National Aeronautics and Space Administration, the U.S. Department of Energy, and Tokyo Electric Power Company. The author would like to thank them for their continued supports on the development of interfacial area transport equation. The author would also like to acknowledge the contributions made by many former and current colleagues.

6. References

[1] G. Kocamustafaogullari, and M. Ishii, "Foundation of the Interfacial Area Transport Equation and Its Closure Relations," *International Journal of Heat and Mass Transfer*, Vol. 38, pp. 481-493, 1995.

[2] M. Ishii, and N. Zuber, "Drag Coefficient and Relative Velocity in Bubbly, Droplet or Particulate Flows," *AIChE Journal*, Vol. 25, pp. 843-55, 1979.

[3] M. Ishii, and S. Kim, "Development of One-Group and Two-Group Interfacial Area Transport Equation," *Nuclear Science and Engineering*, Vol. 146, pp. 257-273, 2004.

[4] X. Sun, S. Kim, M. Ishii, and S. G. Beus, "Modeling of Bubble Coalescence and Disintegration in Confined Upward Two-Phase Flow," *Nuclear Engineering and Design*, Vol. 230, pp. 3-26, 2004.

[5] M. Ishii, and T. Hibiki, *Thermo-Fluid Dynamics of Two-Phase Flow, Second Edition*, New York: Springer, 2010.

[6] I. Kataoka, M. Ishii, and A. Serizawa, "Local Formulation and Measurements of Interfacial Area Concentration in Two-Phase Flow," *International Journal of Multiphase Flow*, Vol. 12, pp. 505-29, 1986.

[7] J. M. Le Corre, E. Hervieu, M. Ishii, and J. M. Delhaye, "Benchmarking and Improvements of Measurement Techniques for Local-Time-Averaged Two-Phase Flow Parameters," *Experiments in Fluids*, Vol. 35, pp. 448-458, 2003.

[8] T. Hibiki, S. Hogsett, and M. Ishii, "Local Measurement of Interfacial Area, Interfacial Velocity and Liquid Turbulence in Two-Phase Flow," *Nuclear Engineering and Design*, Vol. 184, pp. 287-304, 1998.

[9] S. Kim, X. Y. Fu, X. Wang, and M. Ishii, "Development of the Miniaturized Four-Sensor Conductivity Probe and the Signal Processing Scheme," *International Journal of Heat and Mass Transfer*, Vol. 43, pp. 4101-4118, 2000.

[10] T. Hibiki, and M. Ishii, "Interfacial Area Transport Equations for Gas-Liquid Flow," *The Journal of Computational Multiphase Flows*, Vol. 1, pp. 1-22, 2009.

[11] X. Yang, J. P. Schlegel, S. Paranjape, Y. Liu, S. W. Chen, T. Hibiki, and M. Ishii, "Interfacial Area Transport in Two-Phase Flows in a Scaled 8x8 Rod Bundle Geometry at Elevated Pressures," in *The 14th International Topical Meeting on Nuclear Reactor Thermal Hydraulics (NURETH-14)*, Toronto, Ontario, Canada, 2011.

[12] M. Ishii, S. Kim, X. Sun, and T. Hibiki, "Interfacial Area Transport Equation and Implementation into Two-Fluid Model," *Journal of Thermal Science and Engineering Applications*, Vol. 1, pp. 1-7, 2009.

[13] W. Yao, and C. Morel, "Volumetric Interfacial Area Prediction in Upward Bubbly Two-Phase Flow," *International Journal of Heat and Mass Transfer*, Vol. 47, pp. 307-328, 2004.

[14] G. H. Yeoh, and J. Y. Tu, "Population Balance Modelling for Bubbly Flows with Heat and Mass Transfer," *Chemical Engineering Science*, Vol. 59, pp. 3125-3139, 2004.

[15] B. G. Huh, D. J. Euh, H. Y. Yoon, B. J. Yun, C. H. Song, and C. H. Chung, "Mechanistic Study for the Interfacial Area Transport Phenomena in an Air/Water Flow Condition by Using Fine-Size Bubble Group Model," *International Journal of Heat and Mass Transfer*, Vol. 49, pp. 4033-4042, 2006.

[16] X. Wang, and X. Sun, "CFD Simulation of Phase Distribution in Adiabatic Upward Bubbly Flows Using Interfacial Area Transport Equation," in *Proceedings of the 12th International Topical Meeting on Nuclear Reactor Thermal-Hydraulics (NURETH-12)*, Pittsburgh, PA, 2007.

[17] X. Wang, and X. Sun, "Effects of Non-Uniform Inlet Conditions and Lift Force on Prediction of Phase Distribution in Upward Bubbly Flows with Fluent-IATE," in *Proceedings of the 7th International Topical Meeting on Nuclear Reactor Thermal Hydraulics, Operation and Safety (NUTHOS-7)*, Seoul, Korea, 2008.